A Multi-Layer Control Scheme for a Centralized UAV Formation

Alexandre S. Brandão[1], João P. A. Barbosa[1], Valentín Mendoza[2], Mário Sarcinelli-Filho[3] and Ricardo Carelli[4]

Abstract— **This paper presents an application of the multi-layer control scheme to guide a formation of three unmanned aerial vehicles (UAV) in trajectory tracking missions. In such case, each part of the formation control problem is dealt by an individual layer, which is independent module dealing with a specific part of the navigation problem. These layers are responsible to generate the desired path of the formation, to provide the desired posture of the robots, and to establish the control signal of each robot to reach their desired positions. The formation controller here introduced is able to coordinate the robots to the desired formation, including the possibility of time-varying position and/or shape, while a nonlinear underactuated controller previously proposed is responsible to guide the UAVs to their desired positions. The stability analysis of the closed-loop system is demonstrated in the sense of Lyapunov, resulting that the formation errors are ultimately bounded. Finally, simulation results for a group of three quadrotors are presented and discussed to validate the proposed model and controller.**

I. INTRODUCTION

In the last decade, several researches in cooperative navigation control of multiple unmanned aerial vehicles (MUAVs) have been receiving attention of the scientific community. The growing potential for both civilian and military applications justifies the research interest in this area. For tasks that involve environments with large dimension, it is known that a group of UAVs working together in a cooperative way is more advantageous than a unique specialized robot. For instance, search and rescue operation, in which a platoon should cover a large area in a short period of time [1]; seeking a moving target [2]; load transportation task, in which a team should stabilize and move an object from a place to another (in this case, the dimension of the object can make impossible the task execution by only one robot) [3] or in which a team of UAV equipped with grippers should pick up, transport, and assemble the structural elements [4]; area coverage surveillance [5], [6]; infra-structure maintenance; observation of natural risks [7]; inspection of large areas in public safety applications [8], and so on.

In these cases the challenge has been to control the formation of MUAVs, in order to execute a task efficiently in terms a function cost, e.g., formation error, time spent, energy consumption, among others. Therefore there are many ways to approach the formation control problem, however most of them can be included at least in one of three formation structures: leader-follower, behavior-based or virtual structure [9]. In the leader-follower strategy, the robot labeled leader is responsible to guide (or to provide some remarkable information to) the others robots, labeled followers. In the case where the robots should establish a geometric pattern, which moves in the 3-D space, a virtual structure strategy is more reasonable. Finally when the robots should move according to a set of predefined missions (which are selected depending of the current scenario), a behavior-based strategy is commonly adopted.

After choosing the formation structure, one should define the control architecture to be used, which can be centralized or decentralized one. The difference between them is that the first one has a main unit responsible to get information about the whole formation and to solve the navigation problem. In contrast, in the second one the robots use their own information to observe the environment and to react in order to accomplish the predefined mission.

In [10] a leader-follower formation is implemented introducing the concepts of Virtual Body Frame (an equilateral adjustable triangle) for MUAVs. In these opportunity, simulation results highlight how a nonlinear control flight algorithm is able to guide the formation through obstacles (previously identified). Another leader-follower application can be found in [1], where a trajectory tracking strategy for a quadrotor formation is accomplished in the horizontal plane. Sliding mode and linear PD controllers are responsible to guide the translation dynamic and UAV orientation, respectively, and then to preserve the desired formation during real flight experiments. Moreover, a solution for keeping the formation after changing the UAV positions during navigation is presented and validated in [11]. Some improvements of this work are presented in [12], where the focus is to avoid obstacles by rearranging (or regrouping) the UAVs, according to a leader-follower strategy.

The concept of Cluster considering n-robots is presented in [13]. In such case, the displacement of the formation depends on the characteristics of the Cluster Space variables, such as position, orientation and shape. The experimental results using ground robots demonstrate the navigation of the whole formation considering both centralized and decentralized architecture. Despite seeming a strategy based on virtual structure, it can be applied in formations based on leader-follower strategy.

A novel decentralized formation control called Extension-Decomposition-Aggregation (EDA) is introduced in [9] and

[1]A. S. Brandão and J. P. A. Barbosa are with the Department of Electrical Engineering, Universidade Federal de Viçosa, Viçosa - MG, Brazil {alexandre.brandao,joao.p.amorim}@ufv.br

[2]V. Mendoza is with the Department of Mathematics, Universidade Federal de Viçosa, Viçosa - MG, Brazil valentin@ufv.br

[3]M. Sarcinelli-Filho is with the Graduate Program on Electrical Engineering, Federal University of Espírito Santo, Vitória - ES, Brazil mario.sarcinelli@ufes.br

[4]R. Carelli is with the Institute of Automatics, National University of San Juan, San Juan, Argentine rcarelli@inaut.unsj.edu.ar

validated by simulation in [14] to perform a suitable strategy to guide a team of UAVs considering a virtual structure. In order to perform the proposal the team information are used to give the relationship between individual robots and the formation control system, to split them into feasible subsystem individually controlled, and to give the interaction among their subsystems, which, respectively, define the extension, decomposition and aggregation processes. Another virtual structure strategy is implemented in [7] to guide a set of fixed-wing UAVs, which has predefined distances to the virtual leader (in this case a rigid pyramidal structure). The UAVs are controlled in a decentralized way, having a synchronization control strategy responsible to minimize actuator faults, and thus increasing the system robustness.

In our previous work, the Multi-Layer Control Scheme (MLCS) was introduced to guide a *n*-robot ground formation during trajectory tracking mission considering (or not) the absence of obstacles in the environment [15], [16]. Aiming to improve the MLCS capability, the objective of this work is to make it able to guide a 3-D navigation of a MUAVs system. To accomplish it this work is split as following: Section II describes in high-level the UAV dynamic model; Section III briefly presents some comments about the MLCS; Section IV introduces the description of the 3-D formation in order to formalize the formation control layer, and finally, Sections V and VI present some simulation results that validate the proposal, as well as some relevant discussions about them and some concluding remarks about the work.

II. THE DYNAMIC MODEL OF THE ROTORCRAFT

This section presents the rigid-body modeling of a rotorcraft vehicle moving in the 3-D space. According to [17], the whole model of a helicopter/quadrotor can be represented by four interconnected dynamic subsystems, as shown in Fig. 1: the actuator dynamics (responsible for transforming the joystick - or computer generated - commands in servomotor actuation), the rotary-wing dynamics (which embeds the aerodynamic parameters and the thrust generation associated to the main and tail rotors for a helicopter or the four independent motors for a quadrotor), the forces and torques generation (where the thrust force decomposition takes place), and the rigid-body dynamics (which defines the displacement of the rotorcraft in the free Cartesian space).

The two first subsystems, labeled *Low-level Dynamic Model*, can be represented by a linear function, i.e., $\begin{bmatrix} u_\theta & u_\phi & u_\psi & u_{\dot{z}} \end{bmatrix}^T = \alpha \begin{bmatrix} f_1 & f_2 & f_3 & f_4 \end{bmatrix}^T + \beta$, with $\alpha \in \mathbb{R}^4$ and $\beta \in \mathbb{R}^{4 \times 1}$ being constant matrices [18]. The remaining blocks represent the *High-level Dynamic Model*.

In terms of control input notation, u_i represents the real ones (those effectively applied to the UAV), whereas f_i represents the abstract ones (those which cannot be directly applied to the vehicle).

For the interest reader, the UAV dynamic model here used is obtained from the Euler-Lagrange equations in a way quite similar to [19], [20]. However in the context of this work, it is just necessary to define the pose of the rotorcraft in the 3-D space, given by $\mathbf{q} = \begin{bmatrix} \xi & \eta \end{bmatrix}^T$, where

$\xi = \begin{bmatrix} x & y & z \end{bmatrix}^T \in \mathbb{R}^3$, corresponds to the longitudinal, lateral and normal displacements in the inertial frame $\langle g \rangle$, and $\eta = \begin{bmatrix} \phi & \theta & \psi \end{bmatrix}^T \in \mathbb{R}^3$, corresponds to the angles of roll, pitch and yaw with respect to the spatial frame $\langle s \rangle$. for a quadrotor. Fig. 2 illustrates the reference frames and the abstract control inputs f_i. Notice that $\langle s \rangle$ has the same orientation of $\langle g \rangle$, and thus ${}^g\eta \equiv {}^s\eta$. From [21], one gets the dynamic model at the inertial frame $\langle g \rangle$, given by

$$\begin{bmatrix} m\mathbf{I}_3 & \mathbf{0} \\ \mathbf{0} & \mathbf{M}_r \end{bmatrix} \begin{bmatrix} \ddot{\xi} \\ \ddot{\eta} \end{bmatrix} + \begin{bmatrix} \mathbf{0} & \mathbf{0} \\ \mathbf{0} & \mathbf{C}_r \end{bmatrix} \begin{bmatrix} \dot{\xi} \\ \dot{\eta} \end{bmatrix} + \begin{bmatrix} \mathbf{G} \\ \mathbf{0} \end{bmatrix} = \begin{bmatrix} \mathbf{f} \\ \tau \end{bmatrix} - \begin{bmatrix} \mathbf{D}_t \\ \mathbf{D}_r \end{bmatrix}, \quad (1)$$

or simply $\mathbf{M}(\mathbf{q})\ddot{\mathbf{q}} + \mathbf{C}(\mathbf{q}, \dot{\mathbf{q}})\dot{\mathbf{q}} = \tau - \mathbf{D}$, where $\mathbf{I}_3 \in \mathbb{R}^{3 \times 3}$ is an identity matrix, $\mathbf{M}_r(\eta) = W_\eta^T \mathbf{J} W_\eta \in \mathbb{R}^{3 \times 3}$ represents the rotational matrix of inertia, $\mathbf{C}_r(\eta, \dot{\eta}) = \dot{\mathbf{M}}_r - \frac{1}{2}\dot{\eta}^T \frac{\partial \mathbf{M}_r}{\partial \eta} \in \mathbb{R}^{3 \times 3}$ is the rotational matrix of Coriolis and Centripetal forces, and $\mathbf{G} = [0\ 0\ mg]^T$ is the vector of gravitational forces. $\mathbf{D}$ is here included to represent the vector of disturbances and friction forces acting at the rotorcraft, such as the fuselage aerodynamic effects, wind gusts, ground effect, air resistance, and so on.

The whole description about the high-level underactuated nonlinear controller capable to guide a UAV during a 3D flight can be found in our previous work [21]. There it is presented the dynamic model used to represent the rotorcraft, explicitly showing its underactuated character. Following, a suitable controller based on partial feedback linearization is designed for stabilizing the UAV. Moreover, the stability proof of the closed-loop control system is demonstrated in the sense of Lyapunov, including modeled disturbances and parametric errors. Therefore, it is worthy mentioning that such controller will be applied to each UAV to guide it individually to their desired positions.
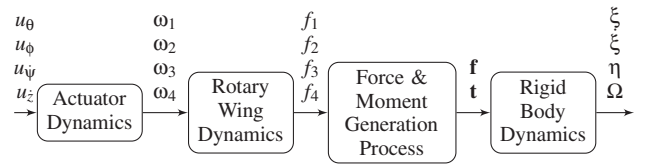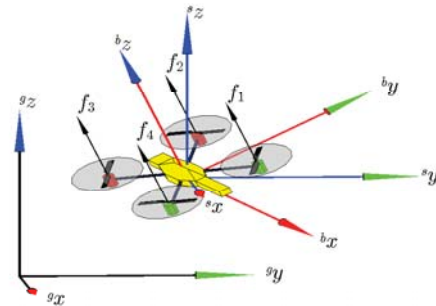

Fig. 1. Block representation of the RUAV dynamics.

Fig. 2. 6-DOF CAD model of a quadrotor, with the reference frames and abstract control inputs f_i associated to them. The inertial, spatial and body frames are denoted by $\langle g \rangle$, $\langle s \rangle$ and $\langle b \rangle$ respectively.

1182

III. THE MULTI-LAYER CONTROL SCHEME

This section briefly describes the Multi-Layer Control Scheme (MLCS) previously proposed in [15] and illustrated in Figure 3. The modules presented in the scheme works independently and deal with each specific part of the problem of formation control, such as the generation of the desired path of the formation, the definition of the desired posture of the robots, and establishment of the control signal of each robot to reach their desired positions.

To give an overview of the MLCS is important to stress the following layers. The first one is the the Off-line Planner Layer, which is responsible to define the initial conditions of the formation, to reshape it (if necessary), and to generate the desired trajectory (or path). In the sequel, there is the Formation Control Layer, which is responsible to provide the control signals for the robots, considering the formation errors, in order to minimize them. It manages the positioning and trajectory tracking strategies. Then, there is the Robot Layer, in which the characteristics of mobile robots are included, such as their kinematic and dynamic configurations, as well as their individual navigation strategies (if exists), such as obstacle avoidance, dynamic compensation, and so on. Finally, the last layer is the Environment, which represents all the objects surrounding the robots, including the relationships between them, like the distance among them to avoid intra-formation collision, for example.

It is important to highlight that an On-line Planner Layer can be included between the Off-liner Planner and Formation Control Layers. It can be useful to deal with formation obstacle avoidance, changing the position or the shape of the formation to prevent collisions, for instance. Such approach is out of scop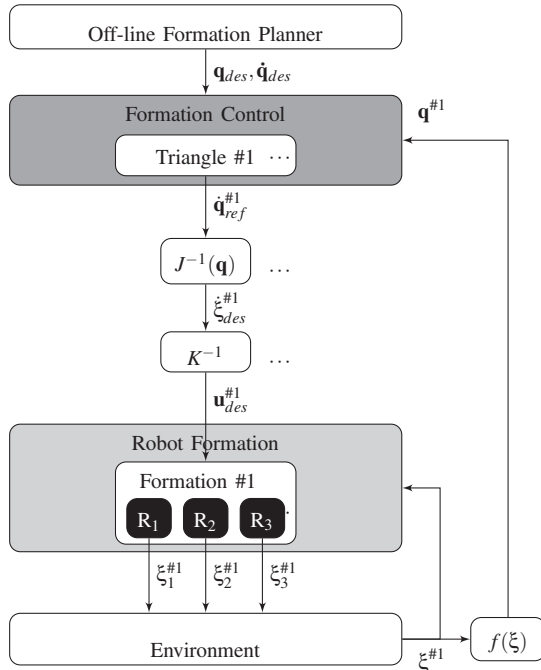e of this work. Some additional comments about the layer independence levels can be found in [15]. Moreover, it is worthy to mention that the MLCS is modular in the horizontal sense, i.e., it grows whenever a new robot is included in the formation (some details can be found in [16] for a formation of ground robots).

It is also important to stress that some additional blocks are necessary to complete the MLCS proposal, such as $J(\cdot)$ and K, which represent the Jacobian matrix and the model of the robot, respectively.

IV. THE FORMATION-CONTROL LAYER

This section presents the Control Layer for a centralized formation control considering three UAVs describing a triangular virtual structure. The state variables used to represent the formation are shown in Fig. 4. The formation pose is defined by $\mathbf{P}_F = [x_F \ y_F \ z_F \ \phi_F \ \theta_F \ \psi_F]^T$ and the structure shape is defined by $\mathbf{S}_F = [p_F \ q_F \ \beta_F]^T$, which represent the distance between R_1 and R_2, the distance between R_1 and R_3, and the angle $R_2\widehat{R_1}R_3$, respectively. It is worthy mentioning that (x_F, y_F, z_F) represents the position of the centroid of the formation.

A. Forward and Inverse Kinematics Transformation

Before introducing the formation control law, it is necessary to express the relationship between the formation pose-shape and the robot positions, as follows

$$\mathbf{P}_F = \begin{bmatrix} \dfrac{x_1 + x_2 + x_3}{3} \\[2mm] \dfrac{y_1 + y_2 + y_3}{3} \\[2mm] \dfrac{z_1 + z_2 + z_3}{3} \\[2mm] \arctan \dfrac{2z_1/3 - z_2/3 - z_3/3}{2y_1/3 - y_2/3 - y_3/3} \\[2mm] -\arctan \dfrac{2z_1/3 - z_2/3 - z_3/3}{2x_1/3 - x_2/3 - x_3/3} \\[2mm] \arctan \dfrac{2y_1/3 - y_2/3 - y_3/3}{2x_1/3 - x_2/3 - x_3/3} \end{bmatrix}, \tag{2}$$
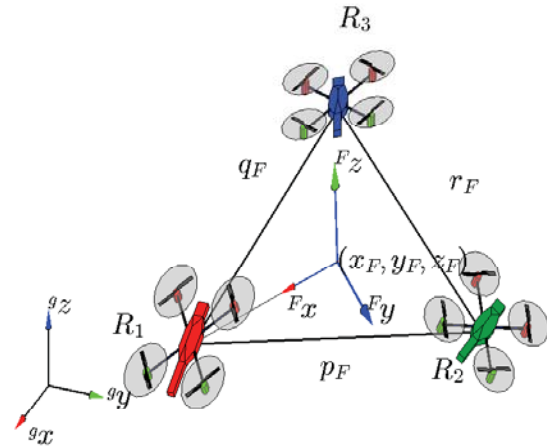

Fig. 3.   Flow diagram of the Multi-Layer Control Scheme.

Fig. 4.   Triangular UAV formation and their state varibles.

1183

$$S_F = \begin{bmatrix} \sqrt{(x_1 - x_2)^2 + (y_1 - y_2)^2 + (z_1 - z_2)^2} \\ \sqrt{(x_1 - x_3)^2 + (y_1 - y_3)^2 + (z_1 - z_3)^2} \\ \arccos \dfrac{p_F^2 + q_F^2 - r_F^2}{2 p_F q_F} \end{bmatrix}, \quad (3)$$

where $r_F = \sqrt{(x_2 - x_3)^2 + (y_2 - y_3)^2 + (z_2 - z_3)^2}$.

Hereinafter, the whole formation will be represented by $\mathbf{q} = [\mathbf{P}_F \ \mathbf{S}_F]^T$ and the robot position by $\xi = [\xi_1 \ \xi_2 \ \xi_3]^T$. It is important to stress that the orientation of the robots is not considered in this proposal. On the other hand, the inverse kinematics transformation is given by

$$\xi = \begin{bmatrix} \mathcal{R} \begin{bmatrix} \frac{2}{3} h_1 \\ 0 \\ 0 \end{bmatrix} + \begin{bmatrix} x_F \\ y_F \\ z_F \end{bmatrix} \\ \mathcal{R} \begin{bmatrix} \frac{2}{3} h_2 \cos(\alpha_1) \\ \frac{2}{3} h_2 \sin(\alpha_1) \\ 0 \end{bmatrix} + \begin{bmatrix} x_F \\ y_F \\ z_F \end{bmatrix} \\ \mathcal{R} \begin{bmatrix} \frac{2}{3} h_3 \cos(\alpha_2) \\ -\frac{2}{3} h_3 \sin(\alpha_2) \\ 0 \end{bmatrix} + \begin{bmatrix} x_F \\ y_F \\ z_F \end{bmatrix} \end{bmatrix}, \quad (4)$$

where

$$\begin{bmatrix} r_F \\ h_1 \\ h_2 \\ h_3 \\ \alpha_1 \\ \alpha_2 \end{bmatrix} = \begin{bmatrix} \sqrt{p_F^2 + q_F^2 - 2 p_F q_F \cos(\beta_F)} \\ \sqrt{\frac{1}{2}(p_F^2 + q_F^2 - \frac{1}{2} r_F^2)} \\ \sqrt{\frac{1}{2}(r_F^2 + p_F^2 - \frac{1}{2} q_F^2)} \\ \sqrt{\frac{1}{2}(q_F^2 + r_F^2 - \frac{1}{2} p_F^2)} \\ \arccos \dfrac{4(h_1^2 + h_2^2) - 9 p_F^2}{8 h_1 h_2} \\ \arccos \dfrac{4(h_1^2 + h_3^2) - 9 q_F^2}{8 h_1 h_3} \end{bmatrix}$$

and

$$\mathcal{R} = \begin{bmatrix} c_\psi c_\theta & c_\psi s_\theta s_\phi - s_\psi c_\phi & c_\psi s_\theta c_\phi + s_\psi s_\phi \\ s_\psi c_\theta & s_\psi s_\theta s_\phi + c_\psi c_\phi & s_\psi s_\theta c_\phi - c_\psi s_\phi \\ -s_\theta & c_\theta s_\phi & c_\theta c_\phi \end{bmatrix}.$$

Notice that h_1 is the distance between $\{R_1\}$ and the central point of the segment $\overline{\{R_2\}\{R_3\}}$, h_2 is the distance between $\{R_2\}$ and the central point of the segment $\overline{\{R_1\}\{R_3\}}$, h_3 is the distance between $\{R_3\}$ and the central point of the segment $\overline{\{R_1\}\{R_2\}}$, all of them passing through (x_F, y_F, z_F).

Taking the first time derivative of the forward and the inverse kinematics transformations we can obtain the relationship between the $\dot{\xi}$ and $\dot{\mathbf{q}}$, represented by the Jacobian matrix, which is given by $\dot{\mathbf{q}} = J(\xi) \dot{\xi}$ in the forward way, and by $\dot{\xi} = J^{-1}(\mathbf{q}) \dot{\mathbf{q}}$ in the inverse way, where

$$J(\xi) = \frac{\partial \mathbf{q}_{n \times 1}}{\partial \xi_{m \times 1}} \quad \text{and} \quad J^{-1}(\mathbf{q}) = \frac{\partial \xi_{m \times 1}}{\partial \mathbf{q}_{n \times 1}},$$

for $m, n = 1, 2, \cdots, 9$.

B. The Formation Controller and its Stability Proof

The Control Layer receives from the upper layer the desired formation pose and shape $\mathbf{q}_d = [\mathbf{P}_{Fd} \ \mathbf{S}_{Fd}]^T$, and its desired variations $\dot{\mathbf{q}}_d = [\dot{\mathbf{P}}_{Fd} \ \dot{\mathbf{S}}_{Fd}]^T$. It generates the pose and shape variation references $\dot{\mathbf{q}}_r = [\dot{\mathbf{P}}_{Fr} \ \dot{\mathbf{S}}_{Fr}]^T$, where the subscripts d and r represent the desired and reference signals, respectively. Defining the formation error as $\tilde{\mathbf{q}} = \mathbf{q}_d - \mathbf{q}$, the proposed formation control law is

$$\dot{\mathbf{q}}_r = \dot{\mathbf{q}}_d + \kappa \tilde{\mathbf{q}}, \quad (5)$$

where κ is a positive definite diagonal gain matrix. Let us consider a difference $\delta_\mathbf{v}$ between the desired and the real formation variations, such as $\dot{\mathbf{q}} = \dot{\mathbf{q}}_{\mathbf{ref}} + \delta_\mathbf{v}$. Then, the closed loop system equation can be written as

$$\dot{\tilde{\mathbf{q}}} + \kappa \tilde{\mathbf{q}} = -\delta_\mathbf{v}. \quad (6)$$

Now, in order to demonstrate the stability of the proposed controller, one can consider the following Lyapunov candidate function

$$V = \frac{1}{2} \tilde{\mathbf{q}}^\mathbf{T} \tilde{\mathbf{q}} > 0,$$

and then, taking its first time derivative, one gets

$$\dot{V} = \tilde{\mathbf{q}}^\mathbf{T} \dot{\tilde{\mathbf{q}}} = -\tilde{\mathbf{q}}^\mathbf{T} \kappa \tilde{\mathbf{q}} - \tilde{\mathbf{q}}^\mathbf{T} \delta_\mathbf{v}.$$

Assuming perfect velocity tracking, $\delta_\mathbf{v} = \mathbf{0}$, and one can conclude that $\dot{V} < 0$, which means that the equilibrium is globally asymptotically stable, i.e., $\tilde{\mathbf{q}} \to \mathbf{0}$ when $t \to \infty$. On the other hand, if $\delta_\mathbf{v}$ is not null, the equilibrium will be asymptotically stable if $\tilde{\mathbf{q}}^\mathbf{T} \kappa \tilde{\mathbf{q}} > |\tilde{\mathbf{q}}^\mathbf{T} \delta_\mathbf{v}|$. A sufficient condition for that is $\|\tilde{\mathbf{q}}\| > \|\delta_\mathbf{v}\| / \lambda_{\min}(\kappa)$, where $\lambda_{\min}(\kappa)$ represents the minimum eigenvalues of κ. That means that the formation error $\tilde{\mathbf{q}}$ is ultimately bounded, and its bound depends on the formation velocity tracking error $\delta_\mathbf{v}$. If a Dynamic Compensation Layer is considered, then $\delta_\mathbf{v}$ can be reduced as shown in [15].

It is important to stress that the nonlinear controller to guide the UAVs to their desired position (computed by the formation controller) is proposed and has its stability analysis demonstrated in [21].

V. RESULTS AND DISCUSSION

This section presents two simulation results considering the proposed controller for trajectory tracking missions. The main objective is to demonstrate the stability of the closed-loop control system during a flight and to check the effectiveness of the controller. The dynamic model of the ArDrone Parrot Inc. is used during the simulations.

The first simulation consists in a growing straight line in x-axis direction and a sinusoidal function in z-axis direction, given by

$$\begin{bmatrix} x_{Fd} \\ y_{Fd} \\ z_{Fd} \end{bmatrix} = \begin{bmatrix} 0.1t \\ 0 \\ 0.5 \sin(0.03\pi t) + 2 \end{bmatrix},$$

while desired pitch angle of the formation continuously grows according to $\theta_{Fd} = 0.02\pi t$. The video available in the

1184

link `http://youtu.be/Jlosdzq1UrM` illustrates this simulation. The formation shape adopted during navigation is $\mathbf{S}_F = [1\ 2\ \pi/4]^T$. The 3-D navigation path and the posture errors during the task execution are shown in Figure 5. One can observe that the absolute positioning errors in $y-$ and $z-$ axes are lower than 50mm. It occurs due to the reference given to the formation, i.e., there is no displacement in $y-$axis, thus the robots maintain the reference once reaching the predefined value. Moreover, considering that the controller in $z-$ direction is almost independent of the other variables, the robots reach faster the reference and remain following it. Now knowing that the UAV horizontal displacement depends directly on the pitch angle, one can notice a higher amplitude of the errors in these variables. In the figure one can note that the formation follows the desired one with a delay in axis. Such steady-state error could be minimized by adding a Dynamic Compensator module in the Multi-Layer Control Scheme.

In the second simulation the formation should track a circle reference with a fixed altitude, while changing its yaw reference. In other words the desired path is given by

$$\begin{bmatrix} x_{Fd} \\ y_{Fd} \\ z_{Fd} \\ \psi_{Fd} \end{bmatrix} = \begin{bmatrix} 4\cos(0.01\pi t) \\ 4\sin(0.01\pi t) \\ 2 \\ 0.02\pi t \end{bmatrix}.$$

The formation shape is $\mathbf{S}_F = [2\ 2\ \pi/3]^T$, defining an equilateral triangle. In such case, the barycenter of the formation could be the object to be escorted by the robots in formation, which circulate around it. During execution of this flight one can image an escort task, as shown in the link `http://youtu.be/eWOZhAjU2tY`.

A similar analysis done for the first simulation can be done for the second one. The most important description to stress is the passive characteristic of x and y variables, which depend directly on the pitch θ and roll ϕ angles, respectively. As explained in [21], taking into account the underactuated aspect of the UAV, these variables are labeled as passive ones in the modeling stage, being governed by the active ones. Thus in Figure 6 one can notice that greater errors (less than 250mm) occur in the xy-plane. Moreover, a following delay can be observed in the time evolution of the 3-D traveled path, which not compromise the accomplishment of the mission. It is known that reducing the angular frequency of the circular reference, the following errors could be smaller. However the aim of this work is to demonstrate the effectiveness of the proposal in these situations.

Other simulations describing a positioning task and a eight-shape reference for trajectory tracking can be found respectively in `http://youtu.be/BUt6_XD8ehs` and in `http://youtu.be/l3e7LLPor8k`. It is worthy to emphasize that the proposal is able to guide a formation during positioning tasks, as well as a set of desired posture and shape is given.

VI. Concluding Remarks

This paper presents an application of the multi-layer control scheme to guide a formation of three unmanned aerial vehicles (UAV) in trajectory tracking missions. The formation controller here proposed is able to coordinate the robots to their desired position, in order to establish the desired formation virtual structure. The possibility of time-varying position and/or shape is also dealt with, which opens the possibility to navigate considering obstacle avoidance strategies.

The nonlinear underactuated controller previously proposed is responsible to guide the UAVs to their desired positions. Thus the stability proof is already demonstrated for a navigation of a UAV during positioning, trajectory tracking and path following mission. In this work, the stability analysis of the closed-loop system is demonstrated in the sense of Lyapunov, resulting that the formation errors are ultimately bounded. The effectiveness of the proposal is validated by simulation results run with a group of three quadrotors, which describes a triangular-shape virtual structure.

The following steps of this work could be to incorporate an obstacle avoidance strategy able to guide safety the whole formation in a semi-structurated environment. Moreover, an adaptive dynamic compensation module could be added in order to reduce the formation errors, thus improving system performance. Finally, in future works we will address the scalability of the proposed scheme to show that it can control a group of n-robots, with different formation shapes. Then, we intend to present some real flight results as soon as we have the equipments (at least three UAVs) to carry out the experiments in our laboratory.
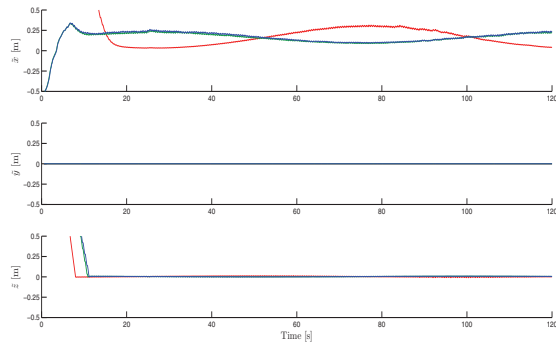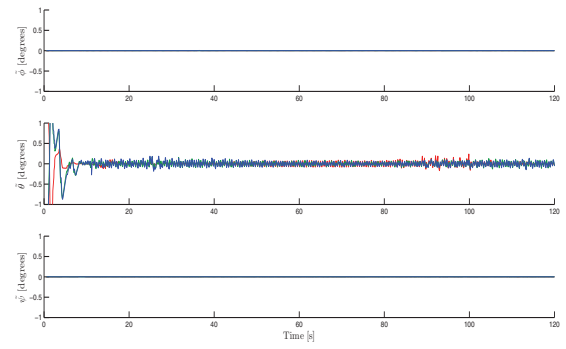
References

[1] D. A. Mercado, R. Castro, and R. Lozano, "Quadrotors flight formation control using a leader-follower approach," in *Proceedings of the 2103 European Control Conference (ECC)*, Zurich, Switzerland, July 17–19 2013, pp. 3858–3863.

[2] S. Zhu, D. Wang, and C. B. Low, "Cooperative control of multiple uavs for moving source seeking," in *Proceedings of the 2013 Internation Conference on Unmanned Aircraft Systems (ICUAS)*, Atlanta, GA, USA, May 28–31 2013, pp. 193–202.

[3] D. Mellinger, M. Shomin, N. Michael, and V. Kumar, "Cooperative grasping and transport using multiple quadrotors," in *Distributed Autonomous Robotic Systems*, ser. Springer Tracts in Advanced Robotics, A. Martinoli, F. Mondada, N. Correll, G. Mermoud, M. Egerstedt, M. A. Hsieh, L. E. Parker, and K. Sty, Eds. Springer Berlin Heidelberg, 2013, vol. 83, pp. 545–558. [Online]. Available: http://dx.doi.org/10.1007/978-3-642-32723-0_39
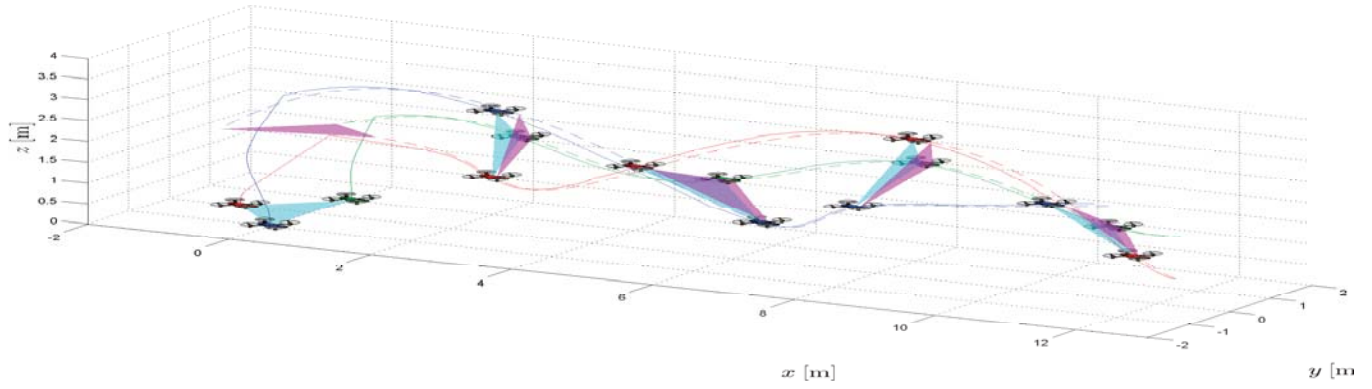
(a) 3-D navigation path.

(b) Position errors.

(c) Angle errors

Fig. 5. Trajectory tracking missing for a MUAVs following a straight line reference using multi-layer control scheme.
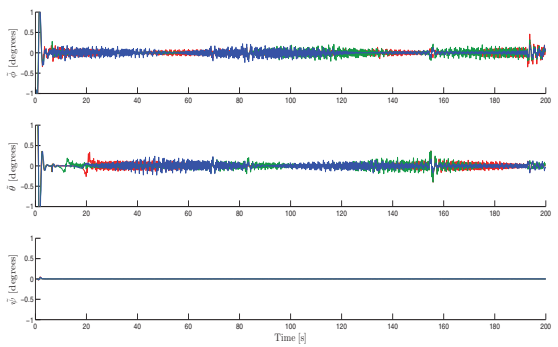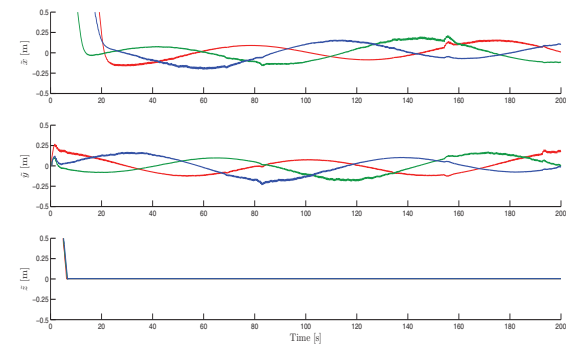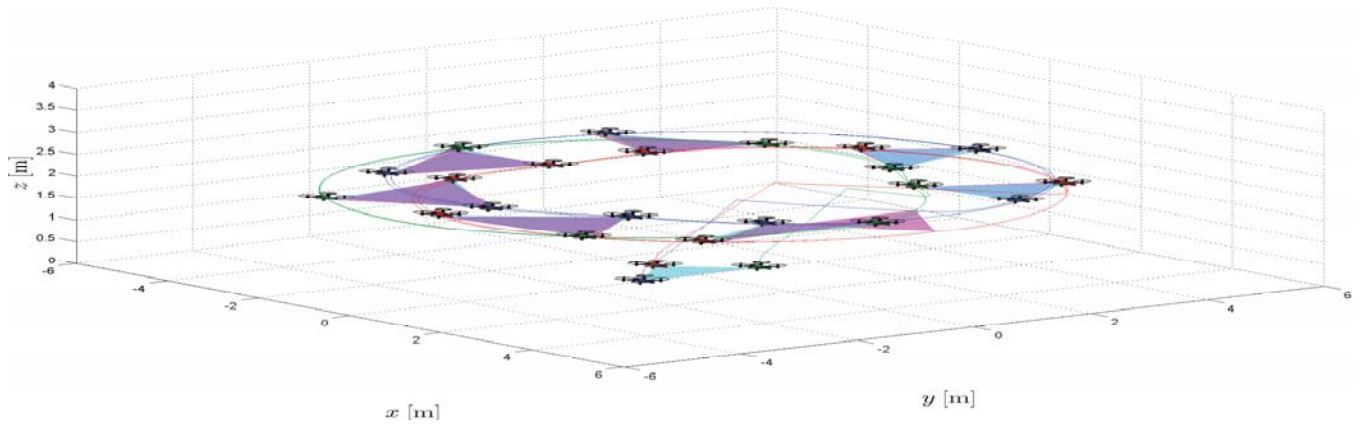

Fig. 6. Trajectory tracking missing for a MUAVs following a circular reference using multi-layer control scheme.

[4] Q. Lindsey, D. Mellinger, and V. Kumar, "Construction with quadrotor teams," *Autonomous Robots*, vol. 33, no. 3, pp. 323–336, 2012. [Online]. Available: http://dx.doi.org/10.1007/s10514-012-9305-0

[5] W. Zheng-Jei and L. Wei, "A solution to cooperative area coverage surveillance for a swarm of muavs," *Internation Journal of Advanced Robotic Systems*, vol. 10, no. 398, pp. 1–8, 2013.

[6] J. Acevedo, B. Arrue, J. Díaz-Báñez, I. Ventura, I. Maza, and A. Ollero, "Decentralized strategy to ensure information propagation in area monitoring missions with a team of uavs under limited communications," in *Proceedings of the 2013 Internation Conference on Unmanned Aircraft Systems (ICUAS)*, Atlanta, GA, USA, May 28–31 2013, pp. 565–574.

[7] H. Rezaee and F. Abdollahi, "A synchronization strategy for three dimensional decentralized formation control of unmanned aircrafts," in *Proceedings of the 37th Annual Conference on IEEE Industrial Electronics Society (IECON 2011)*, Melbourne, Australia, November 7–10 2011, pp. 462–467.

[8] I. Maza, F. Caballero, J. Capitán, J. M. de Dios, and A. Ollero, "Experimental results in multi-uav coordination for disaster management and civil security applications," *Journal of Intelligent and Robotic Systems*, vol. 64, no. 1-4, pp. 563–585, December 2010.

[9] A. Yang, W. Naeem, G. W. Irwin, and K. Li, "Novel decentralized formation control for unmanned vehicles," in *Proceedings of the 2012 Intelligent Vehicles Symposium*, Alcalá de Henares, Spain, June 3–7 2012, pp. 13–18.

[10] X. Shi and J. Yang, "Design of formation flight control based on virtual body frame of the team formation," in *Proceedings of the 25th Chinese Control and Decision Conference (CCDC)*, Guiyang, China, May 25–27 2013, pp. 796–800.

[11] D. Luo, W. Xu, S. Wu, and Y. Ma, "Uav formation flight control and formation switch strategy," in *Proceedings of the 8th International Conference on Computer Science and Education (ICCSE)*, Colombo, Sri Lanka, April 26–28 2013, pp. 264–269.

[12] D. Luo, T. Zhou, and S. Wu, "Obstacle avoidance and formation regrouping strategy and control for uav formation flight," in *Proceedings of the 10th IEEE International Conference on Control and Automation (ICCA)*, Hangzhou, China, June 12–14 2013, pp. 1921–1926.

[13] I. Mas and C. Kitts, "Centralized and decentralized multi-robot control methods using the cluster space control framework," in *Proceedings of the 2010 IEEE/ASME International Conference on Advanced Intelligent Mechatronics*, Montral, Canada, July 6–9 2010, pp. 115–122.

[14] A. Yang, W. Naeem, G. W. Irwin, and K. Li, "A decentralized control strategy for formation flight of unmanned aerial vehicles," in *Proceedings of the UKACC International Conference on Control*, Cardiff, UK, September 3–5 2012, pp. 345–350.

[15] A. S. Brandão, F. N. Martins, V. T. L. Rampinelli, M. Sarcinelli-Filho, T. F. Bastos-Filho, and R. Carelli, "A multi-layer control scheme for multi-robot formations with adaptive dynamic compensation," in *Proceedings of the 5th IEEE International Conference on Mechatronics*. Mlaga, Spain: IEEE, 2009.

[16] V. T. L. Rampinelli, A. S. Brandão, F. N. Martins, M. Sarcinelli-Fillho, and R. Carelli, "Embedding obstacle avoidance in the control of a flexible multi-robot formation," in *Proceedings of the IEEE Internation Symposium on Industrial Electronics*, Bari, Italy, July 4–7 2010.

[17] B. Ahmed, H. R. Pota, and M. Garratt, "Flight control of a rotary wing uav using backstepping," *International Journal of Robust and Nonlinear Control*, vol. 20, pp. 639–658, January 2010.

[18] K. Kondak, M. Bernard, N. Meyer, and G. Hommel, "Autonomously flying vtol-robots: Modeling and control," in *Proceedings of the IEEE International Conference on Robotics and Automation*, Rome, Italy, April 10-14 2007, pp. 736–741.

[19] P. Castillo, R. Lozano, and A. Dzul, *Modelling and Control of Mini-Flying Machines*. USA: Springer, 2005.

[20] G. V. Raffo, M. G. Ortega, and F. R. Rubio, "An integral predictive/nonlinear $\mathcal{H}_\infty$ control structure for a quadrotor helicopter," *Automatica*, vol. 46, pp. 29–39, 2010.

[21] A. S. Brandão, M. Sarcinelli-Filho, and R. Carelli, "High-level under-actuated nonlinear control for rotorcraft machines," in *Proceedings of the IEEE International Conference on Mechatronics*. Vicenza, Itália: IEEE, February 27 – March 1 2013.